JOURNAL OF APPLIED ELECTROCHEMISTRY 19 (1989) 683–696

Investigation of water electrolysis by spectral analysis. I. Influence of the current density*

C. GABRIELLI, F. HUET, M. KEDDAM, A. SAHAR

LP15 du CNRS, Physique des Liquides et Electrochimie, Laboratoire de l'Université Pierre et Marie Curie, Tour 22, 4 Place Jussieu, 75252 Paris Cedex 05, France

Received 28 September 1988; revised 13 February 1989

The potential (or current) fluctuations observed under current (or potential) control during gas evolution were analysed by spectral analysis. The power spectral densities (psd) of these fluctuations were measured for hydrogen and oxygen evolution in acid and alkaline solutions at a platinum disk electrode of small diameter. Using a theoretical model, some parameters of the gas evolution were derived from the measured psd of the potential fluctuations, such as the average number of detached bubbles per time unit, the average radius of the detached bubbles and the gas evolution efficiency. The influence of the electrolysis current on these parameters was also investigated. The results of this first attempt at parameter derivation are discussed.

Nomenclature

b	Tafel coefficient (V^{-1}), Equation 46
C	electrode double layer capacity (F)
e	gas evolution efficiency (%)
f	frequency (Hz)
f_p	frequency of the peak in the psd ψ_v and ψ_i (Hz)
F	Faraday constant, 96487 C mol^{-1}
I	electrolysis current (A)
J	electrolysis current density (mA cm^{-2})
k	slope of the linear potential increase (V s^{-1}), see Fig. 1
n	number of electrons involved in the reaction to form one molecule of the dissolved gas
r_b	radius of a spherical glass ball (m)
r_e	radius of the disk electrode (m)
R_e	electrolyte resistance (Ω)
R_p	polarization resistance (Ω)
R_t	charge transfer resistance (Ω)
u_t	distribution function of the time intervals between two successive bubble departures (s^{-1})
v_g	mean volume of gas evolved per unit time ($m^3\ s^{-1}$)
v_t	gas equivalent volume produced in molecular form per unit time ($m^3\ s^{-1}$)
V_0	gas molar volume, 24.5 × 10^{-3} m^3 at 298 K
x_0	time pseudoperiod of bubbles evolution (s)
Z	electrode electrochemical impedance (Ω)

Greek characters

α_e	dimensionless proportional factor (Equation 19)
β	slope of log λ/log J and log e/log J curves
λ	number of bubbles evolved per unit time (s^{-1})
η_a	activation overpotential (V)
η_{ci}	concentration overpotential of reacting ionic species (V)
η_{cs}	concentration overpotential of dissolved molecular gas (V)
η_{ohm}	ohmic overpotential (V)
η_t	total overpotential (V)
ν	parameter characteristic of the gas evolution pseudoperiodicity, Equation 13 (s^{-1})
τ	time constant of the double layer capacity change (s)
ψ_v	power spectral density (psd) of the potential fluctuations ($V^2\ Hz^{-1}$)
ψ_i	power spectral density (psd) of the current fluctuations ($A^2\ Hz^{-1}$)

Special symbols

$\overline{\eta_j}$	spatial average of the overpotential η_j over the electrode surface
$\overline{\eta_{j,o}}$	time averaged value of $\overline{\eta_j}$
$\Delta\eta_j$	fluctuation of $\overline{\eta_j}$ around $\overline{\eta_{j,o}}$
$\langle\Delta\eta\rangle$	mean value of the total overpotential jump amplitude due to a bubble departure
$\langle\Delta I\rangle$	mean value of the current jump amplitude due to a bubble departure

1. Introduction

Electrolytically generated bubbles induce an increase of the electrode overpotential under current control. The literature is mainly concerned with the ohmic drop increase [1–4]; only recently Leistra and Sides [5] and Dukovic and Tobias [6] detailed the three components of the overpotential increase: ohmic, kinetic and concentration effects.

The overpotentials given in the literature are time

* Paper presented at the 2nd International Symposium on Electrolytic Bubbles organized jointly by the Electrochemical Technology Group of the Society of Chemical Industry and the Electrochemistry Group of the Royal Society of Chemistry and held at Imperial College, London, 31st May and 1st June 1988.

0021-891X/89 $03.00 + .12

averaged values; around these values fluctuations can be observed, which are due to the continuous change of the bubble configuration on the electrode. Though the fluctuation analysis can *a priori* give information on bubble evolution at an elementary level (birth, growth and detachment of a bubble), only a few studies concerning fluctuations have been reported [7, 8].

The potential difference between a gas evolving working electrode (WE) and a reference electrode (RE) can be written [5] at a given time, t (that means for a given bubble configuration)

$$V_{WE} - V_{RE} = E_0 + \eta_t(t) \quad (1)$$

where E_0 is the equilibrium potential without the bubbles and η_t is the total overpotential given by

$$\eta_t(t) = \overline{\eta_{ohm}}(t) + \overline{\eta_a}(t) + \overline{\eta_{cs}}(t) + \overline{\eta_{ci}}(t) \quad (2)$$

$\overline{\eta_{ohm}}$, $\overline{\eta_a}$, $\overline{\eta_{cs}}$, $\overline{\eta_{ci}}$ represent the spatial averages over the electrode surface necessary to take into account the non-uniform current distribution of the ohmic drop, the activation overpotential and the concentration overpotentials of supersaturated dissolved molecular gas and reacting ionic species, respectively. These four terms depend on time, t, and therefore fluctuate so long as the bubbles evolve; they can be expressed by

$$\overline{\eta_j}(t) = \overline{\eta_{j,o}} + \Delta\eta_j(t) \quad (3)$$

where the four terms $\Delta\eta_j(t)$ represent the overpotential fluctuations around the d.c. components $\overline{\eta_{j,o}}$ which are time-averaged values.

The total overpotential, η_t, usually reported in the literature is then

$$\eta_t = \overline{\eta_{ohm,o}} + \overline{\eta_{a,o}} + \overline{\eta_{cs,o}} + \overline{\eta_{ci,o}} \quad (4)$$

In a previous paper [9] it has been shown that under current control the overpotential fluctuations, $\Delta\eta_{ohm}$ and $\Delta\eta_a$, can be written in terms of resistance fluctuations

$$\Delta\eta_{ohm}(t) = \Delta R_e(t)I \quad (5)$$

$$\Delta\eta_a(t) = \Delta R_p(t)I \quad (6)$$

where I is the electrolysis current and ΔR_e and ΔR_p are the fluctuating parts of the electrolyte resistance, R_e, and the polarization resistance (low frequency limit of the impedance), R_p, which reduces to the charge transfer resistance R_t when the reaction mechanism of dissolved molecular gas production is a simple charge transfer reaction. The impedance variation induced by the presence on the electrode surface of an insulating sphere simulating a bubble has been measured for an iron disk electrode in sulphuric acid close to the corrosion potential. This showed that the resistance increments ΔR_e and ΔR_p are proportional to the square of the sphere diameter, i.e. to the projected area of the sphere and, therefore, could be interpreted as a screening effect of the electrode active surface. Consequently, during gas evolution the fluctuating terms $\Delta\eta_{ohm}$ and $\Delta\eta_a$ can be viewed as induced by the electrode active surface fluctuations.

Viewed simply, the total overpotential fluctuations have two origins: first, the electrode active surface fluctuations (leading to $\Delta\eta_{ohm}$ and $\Delta\eta_a$) and, second, the concentration overpotential fluctuations (leading to $\Delta\eta_{cs}$ and $\Delta\eta_{ci}$) when the electrolyte motion due to the bubble growth and departure provokes a change in the concentration gradients of the dissolved gas or reacting ions in the vicinity of the electrode surface.

In this paper the gas evolution experimental conditions (mainly high electrolysis current density and relatively high H^+ or OH^- concentration) are such that the overpotential fluctuations are induced by the electrode active surface fluctuations while the concentration overpotential fluctuations are negligible. In other experimental conditions these latter effects can be predominant [10, 11]. The total overpotential fluctuation is now expressed by

$$\Delta\eta_t(t) = \Delta\eta_{ohm}(t) + \Delta\eta_a(t) \quad (7)$$

and can be studied either in the time domain (measurement of the correlation function or statistical counting if the potential transients are distinguishable) or, as in this paper, in the frequency domain (measurement of the power spectral density which is the Fourier transform of the correlation function). It will be shown for water electrolysis on a platinum disk electrode in acid or alkaline media how the psd (also called the spectrum) of the potential fluctuations allows some parameters of the gas evolution to be estimated, such as the bubble detachment mean radius, the mean number of bubbles evolved per unit time and, consequently, the gas evolution efficiency.

Up to now only potential fluctuations have been mentioned; if the gas-evolving electrode is polarized under potential control, fluctuations of the electrolysis current can be observed. The psd of these current fluctuations has also been measured and it will be pointed out that the same kind of information can be obtained from the current fluctuation spectrum or from the potential fluctuation spectrum.

2. Model and parameter calculation

Time recordings of (over)potential fluctuations have already been published [7, 8] (see also Fig. 4) and can be modelled as in Fig. 1. The steep potential jumps are related to the detachment of bubbles from the electrode, whereas the linear potential increase is due to the bubble growth, as shown in [9] from a theoretical calculation when there are a few bubbles on the electrode and when their growth is controlled by dissolved molecular gas diffusion. We must insist upon the fact that this linear potential increase is due to the growth of all the bubbles on the electrode, i.e. its duration does not represent the lifetime of one bubble, as previously thought in [8].

The psd of the modelled potential fluctuations will now be given (for details about the calculation method and hypothesis, see [10, 12]) and it will be shown how to estimate the number, λ, of bubbles evolved per unit time, and the mean value, $\langle\Delta\eta^2\rangle$, of the square of the

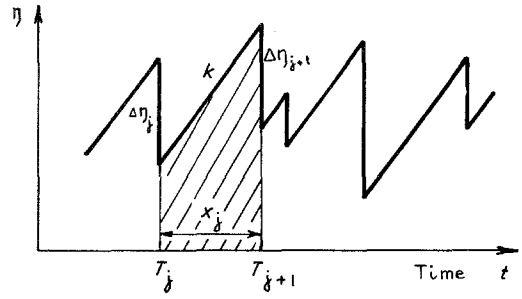

Fig. 1. Theoretical potential fluctuations characteristic of a gas evolution (the elementary transient is hatched): $\Delta\eta_j$ is the potential jump due to the bubble departure at time T_j.

potential jump amplitude due to bubble detachment. Then the mean radius, $\langle r_d \rangle$, of bubble detachment and the gas evolution efficiency, e, will be derived from λ and $\langle \Delta\eta^2 \rangle$.

2.1. *Theoretical psd*

The point process defined by the detachment times of the bubbles from the electrode is supposed to be a renewal process [13, 14], i.e. the sequence of the time intervals x_j, between two successive bubble departures is a sequence of independent random variables with the same distribution function, $u_1(x)$

$$u_1(x) = \frac{d}{dx}(\text{Prob}\ (x_j < x)) \tag{8}$$

Two cases are examined successively.

2.1.1. Exponential distribution function. When there are many more short time intervals, x_j, than long ones (see Fig. 4a), $u_1(x)$ is supposed to be an exponential function

$$u_1(x) = \lambda e^{-\lambda x} \tag{9}$$

The mean value of the potential jump amplitudes is then expressed by

$$\langle \Delta\eta \rangle = \frac{k}{\lambda} \tag{10}$$

where k is the slope of the linear potential increase (see Fig. 1), and the psd of the potential fluctuations is given, for the frequency f ($f \geqq 0$), by

$$\psi_v(f) = \frac{2\lambda\langle \Delta\eta^2 \rangle}{\lambda^2 + 4\pi^2 f^2} \tag{11}$$

which is plotted in Fig. 2. The plateau in the low frequency range is followed by a decrease in f^{-2} in the high frequency range where the psd is equivalent ($\sim$) to

$$\psi_v(f) \sim \frac{\lambda\langle \Delta\eta^2 \rangle}{2\pi^2 f^2} \quad \text{for } f \gg \frac{\lambda}{2\pi} \tag{12}$$

From the low frequency limit $\psi_v(0)$ and the psd value $\psi_v(f)$ at a given frequency, f, in the high frequency range, the parameters λ and $\langle \Delta\eta^2 \rangle$ can be derived.

It must be noticed that a renewal process with an exponential distribution function of the time intervals x_j is simply a Poisson process. However, the calculation of the psd cannot be done as easily as in [8] with the filtered Poisson process theory, since this theory assumes the independence of the random parameters characterizing the potential transient (lifetime of the transient, jump amplitude, etc.) whereas for the modelled potential fluctuations of Fig. 1, the lifetime of the potential transient is equal to (i.e. strongly depends on) the time interval x_j between two successive bubble departures [12].

2.1.2. Pseudoperiodical distribution function. When the bubble detachment is nearly periodic (see Fig. 4b), $u_1(x)$ can be expressed as

$$u_1(x) = \frac{\nu}{2 - e^{-\nu x_0}} \exp\ (-\nu|x - x_0|) \tag{13}$$

where x_0 is the time pseudoperiod and ν (expressed in s^{-1}) represents the more or less pronounced character of the pseudoperiodicity (a periodicity should be given by $u_1(x) = \delta(x - x_0)$ where $\delta(x)$ is the Dirac

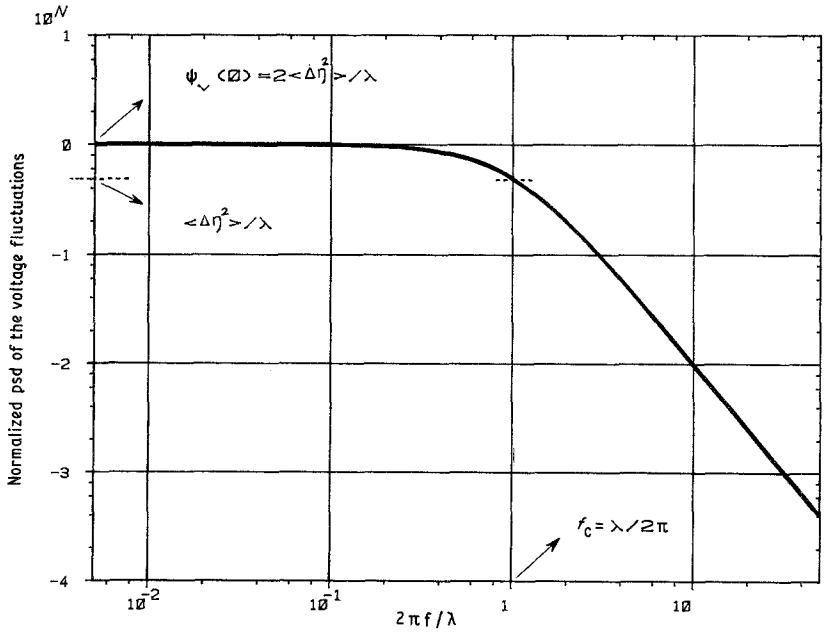

Fig. 2. Theoretical normalized psd of the voltage fluctuations given in Fig. 1 in the case of an exponential distribution function $u_1(x)$ of the time interval between T_j and T_{j+1}.

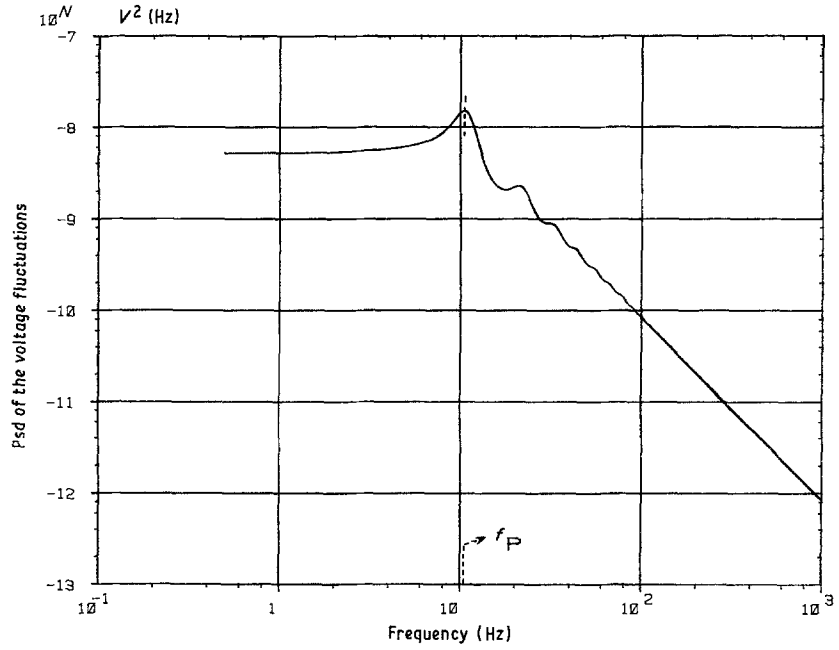

Fig. 3. Theoretical psd of the voltage fluctuations given in Fig. 1 in the case of a pseudoperiodical distribution function $u_1(x)$. The psd is calculated for oxygen evolution in H_2SO_4 (Fig. 5B, spectrum d): $k = 13\,\mathrm{mV\,s^{-1}}$, $x_0 = 0.09\,\mathrm{s}$, $\nu = 50\,\mathrm{s^{-1}}$, $\langle\Delta\eta^2\rangle = 1.07\,\langle\Delta\eta\rangle^2$.

function). The number of bubbles evolved per unit time is then

$$\lambda = \frac{1}{\langle x\rangle} \approx \frac{1}{x_0} \tag{14}$$

and the mean value of the potential jump amplitudes can be written

$$\langle\Delta\eta\rangle = k\langle x\rangle \approx kx_0 \tag{15}$$

The psd, calculated for a linear potential transient, is plotted in Fig. 3. This spectrum shows a plateau in the low frequency range, a peak at a frequency f_p, more or less pronounced, with possible harmonics and a decrease in f^{-2} in the high frequency range given again by Equation 12

$$\psi_v(f) \sim \frac{\lambda\langle\Delta\eta^2\rangle}{2\pi^2 f^2} \quad \text{for } f \gg f_p \tag{16}$$

where the peak frequency, f_p, is related to the number, λ, of bubbles evolved per unit time

$$f_p = \frac{1}{\langle x\rangle} = \lambda \tag{17}$$

It can be shown [10, 12] that the high frequency decrease in f^{-2} comes from the fact that the potential jumps due to bubble detachments are steep. Furthermore Equations 12 and 16 are valid whatever the distribution function and whatever the shape (linear or not) of the potential transient (ending again with a steep jump) may be.

Hence, for pseudoperiodical gas evolution (which is often encountered with small electrodes), even if the potential transient is not linear, the determination of λ and $\langle\Delta\eta^2\rangle$ from the measured psd of the potential fluctuations with Equations 16 and 17 is perfectly correct.

2.2. *Determination of* $\langle r_d\rangle$ *and e*

As the bubble detachment is assumed to be instantaneous and the secondary potential distribution [9] does not have time to build up, the amplitude, $\Delta\eta$, of the induced potential jump is related to the electrolyte resistance variation, ΔR_e, due to the bubble departure, i.e. according to Equation 5

$$\Delta\eta = \Delta\eta_{ohm} = \Delta R_e I \tag{18}$$

where I is the electrolysis current.

It has been shown [9] that the electrolyte resistance variation ΔR_e due to the presence of an insulating sphere simulating a bubble on the electrode surface varies as

$$\frac{\Delta R_e}{R_e} = \alpha_e\left(\frac{r_b}{r_e}\right)^2 \tag{19}$$

where r_b and r_e are the sphere and disk electrode radii, respectively and α_e is a proportionality coefficient independent of r_b and r_e but depending only upon geometrical considerations (disk electrode and sphere placed on the electrode center). The value of α_e has been estimated from impedance measurements in the case of an iron disk electrode in sulfuric acid close to the corrosion potential

$$\alpha_e \simeq 0.4 \tag{20}$$

If the electrolyte resistance variation, ΔR_e, due to the departure of a bubble with detachment radius r_d is supposed to be given by Equation 19, then the amplitude, $\Delta\eta$, of the induced potential jump can be written by using Equation 18

$$\Delta\eta = R_e I\alpha_e\left(\frac{r_d}{r_e}\right)^2 \tag{21}$$

where R_e is now the electrolyte resistance of the

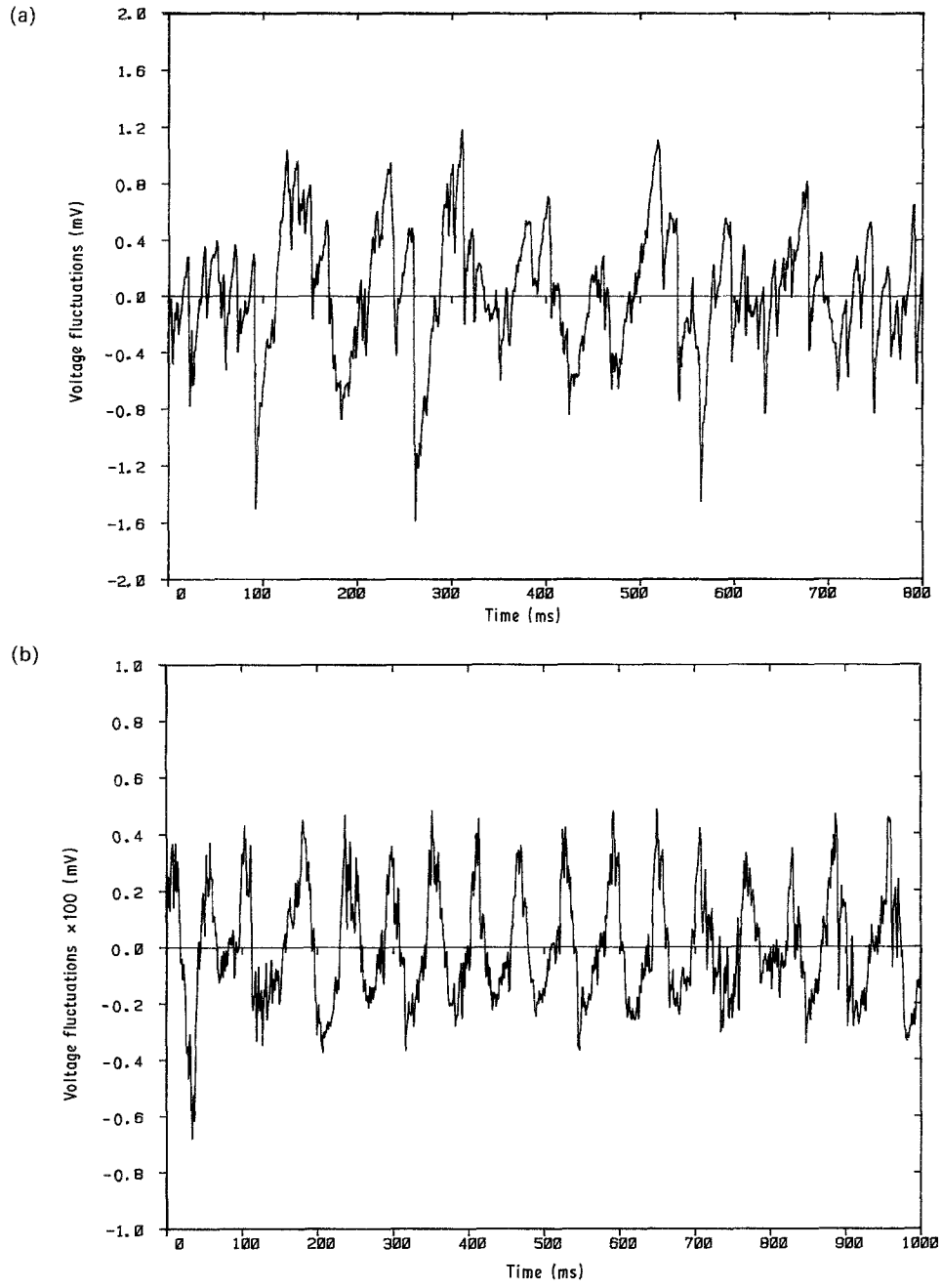

Fig. 4. Time recording of the voltage fluctuations induced by hydrogen evolution on a platinum disk electrode (diameter 0.5 mm) facing upwards in 1 M H_2SO_4 (a) current density $J = 380\,\mathrm{mA\,cm^{-2}}$; (b) current density $J = 7.1\,\mathrm{A\,cm^{-2}}$.

electrode with the bubbles still present on its surface. $\Delta\eta$, like r_d, is a random quantity and its mean value can be expressed from Equation 21 by

$$\langle \Delta\eta \rangle = \frac{R_e I \alpha_e}{r_e^2} \langle r_d^2 \rangle \tag{22}$$

In order to calculate the mean value, $\langle r_d \rangle$, of the bubble detachment radius from the quantity $\langle \Delta\eta^2 \rangle$ estimated from the measured psd of the potential fluctuations, the following approximations are supposed

$$\langle \Delta\eta \rangle \simeq \sqrt{\langle \Delta\eta^2 \rangle} \tag{23}$$

$$\langle r_d \rangle \simeq \sqrt{\langle r_d^2 \rangle} \tag{24}$$

These approximations, which appear to be surprising at first sight, can be considered as valid for the small gas-evolving electrodes used in this work, where the bubble detachment is often pseudoperiodic. As a matter of fact if the gas evolution were actually periodic, the bubble detachment radius, r_d, and the induced potential jump, $\Delta\eta$, would not be random quantities, so that Equations 23 and 24 would become strict equalities. Furthermore, even in the case of Fig. 4a where the gas evolution is not at all periodic and the jump amplitudes are very different (ratio of the largest one over the smallest one equal to 70), it can be shown from statistical counting that

$$\langle \Delta\eta \rangle \simeq 0.65\sqrt{\langle \Delta\eta^2 \rangle} \tag{25}$$

Then in this case, which can be considered as the worst one, Equation 23 represents an overestimate of $\langle \Delta\eta \rangle$ of 53%, which will be accepted in this first attempt at estimation of the gas evolution parameters $\langle r_d \rangle$ and e.

The mean value of the bubble detachment radius $\langle r_d \rangle$ is then given by Equations 22, 23 and 24

$$\langle r_d \rangle = \frac{r_e \langle \Delta\eta^2 \rangle^{1/4}}{(R_e I \alpha_e)^{1/2}} \quad (26)$$

The mean volume, v_g, of gas evolved per unit time can be written

$$v_g = \lambda \tfrac{4}{3}\pi \langle r_d^3 \rangle \quad (27)$$

or

$$v_g = \lambda \tfrac{4}{3}\pi \langle r_d \rangle^3 \quad (28)$$

with the same approximation as in Equation 24. The equivalent volume, v_t, of gas produced in molecular form per unit time is given by Faraday's law

$$v_t = \frac{I V_0}{nF} \quad (29)$$

where I is the electrolysis current, V_0 is the molar volume ($V_0 \simeq 24.51$ at 298 K if the gas pressure in the bubbles is supposed to be near 1 atm), n is the number of electrons involved in the gas production reaction ($n = 2$ for hydrogen and $n = 4$ for oxygen) and F is the Faraday number.

The gas evolution efficiency, e, which represents the amount of produced molecular gas evolved in bubble form, can then be expressed by

$$e = \frac{v_g}{v_t} = \tfrac{4}{3}\pi \frac{nF}{V_0} \frac{\lambda \langle r_d \rangle^3}{I} \quad (30)$$

The gas evolution efficiency can then be easily estimated from the psd of the potential fluctuations.

3. Experimental details

The measurements were performed at room temperature in a one-compartment cylindrical cell where the gas-evolving electrode was located close to an optical window made through the lateral surface of the cell. This window was used for observing the gas evolution on the electrode with a binocular microscope; the electrode surface was horizontal and facing upwards in order to facilitate the release of the gas bubbles.

The working electrode was the cross section of a platinum rod of diameter 0.5 mm embedded in glass. Its surface was carefully polished, first with an emery paper (grade 1200) then with a 6 μm diamond paste so as to prevent the formation of crevices at the metal–glass junction which give rise to evolution of bubbles larger than those evolving on the electrode surface itself, especially at low current density.

The counter-electrode was a platinum grid of large surface. The electrolyte was either sulphuric acid 1 M or sodium hydroxide (1 M) aqueous solution made from bidistilled water. The reference electrode was of the saturated mercurous sulphate type in sulphuric medium and of the saturated calomel type in alkaline medium.

Gas evolution was studied for electrolysis current densities ranging from 50 mA cm^{-2} to 9 A cm^{-2}. Lower values of the current density could not be used with the one-compartment cell, probably because the concentration of the dissolved molecular gas was not well defined and induced a drift of the electrode potential (under current control) which perturbed the measurement of the psd of the low-level potential fluctuations.

The experimental arrangements used for measuring the potential fluctuation psd in galvanostatic control and the current fluctuation psd in potentiostatic control have already been described [8, 15]. The spectrum analyser (Hewlett–Packard 5451C) used a fast Fourier transform algorithm.

4. Results and discussion

4.1. *Potential fluctuations*

Typical time recordings of the potential fluctuations measured during hydrogen evolution in sulphuric acid are shown in Fig. 4: at a low current density (curve a) there are many more short time intervals between two successive bubble detachments than long ones, whereas at a higher current density (curve b) the bubble detachment is nearly periodical.

These recordings show roughly the linear time evolution of the potential followed by a steep jump due to a bubble detachment: in other experimental conditions the shape of the potential fluctuations is sometimes more complicated and the potential jump is not so steep, in particular in the case when the bubble still has an influence on the electrode potential after its detachment.

From these time recordings a statistical analysis of the number and the amplitude of the potential jumps gives the detached bubble frequency, λ, and a histogram of the potential jump amplitude, from which, as explained in Section 2, a histogram of the bubble detachment radius, and then the mean value $\langle r_d \rangle$ of the bubble detachment radius, can be derived.

This statistical method seems rather complicated, especially if only the quantity $\langle r_d \rangle$ is desired, and often difficult to apply when the bubbles are so numerous that the potential transients are hardly distinguishable. Furthermore this technique assumes that the potential fluctuations are induced by the fluctuations of the electrode active surface, which is not the case in some experimental conditions when the fluctuations of the concentration overpotential are no longer negligible.

In this paper we have preferred to work in the frequency domain for the following reasons: in this domain the different phenomena occurring on the gas-evolving electrode can sometimes be identified on the psd curve when their contributions are not in the same frequency range. For example, Fig. 6a shows a spectrum with two plateaux followed by a decrease revealing two phenomena inducing fluctuations on the electrode. Besides, as shown in Section 2, the gas evolution parameters $\langle r_d \rangle$ and e are easily derived from the measured psd.

The psd of the potential fluctuations measured on a hydrogen- and an oxygen-evolving electrode have

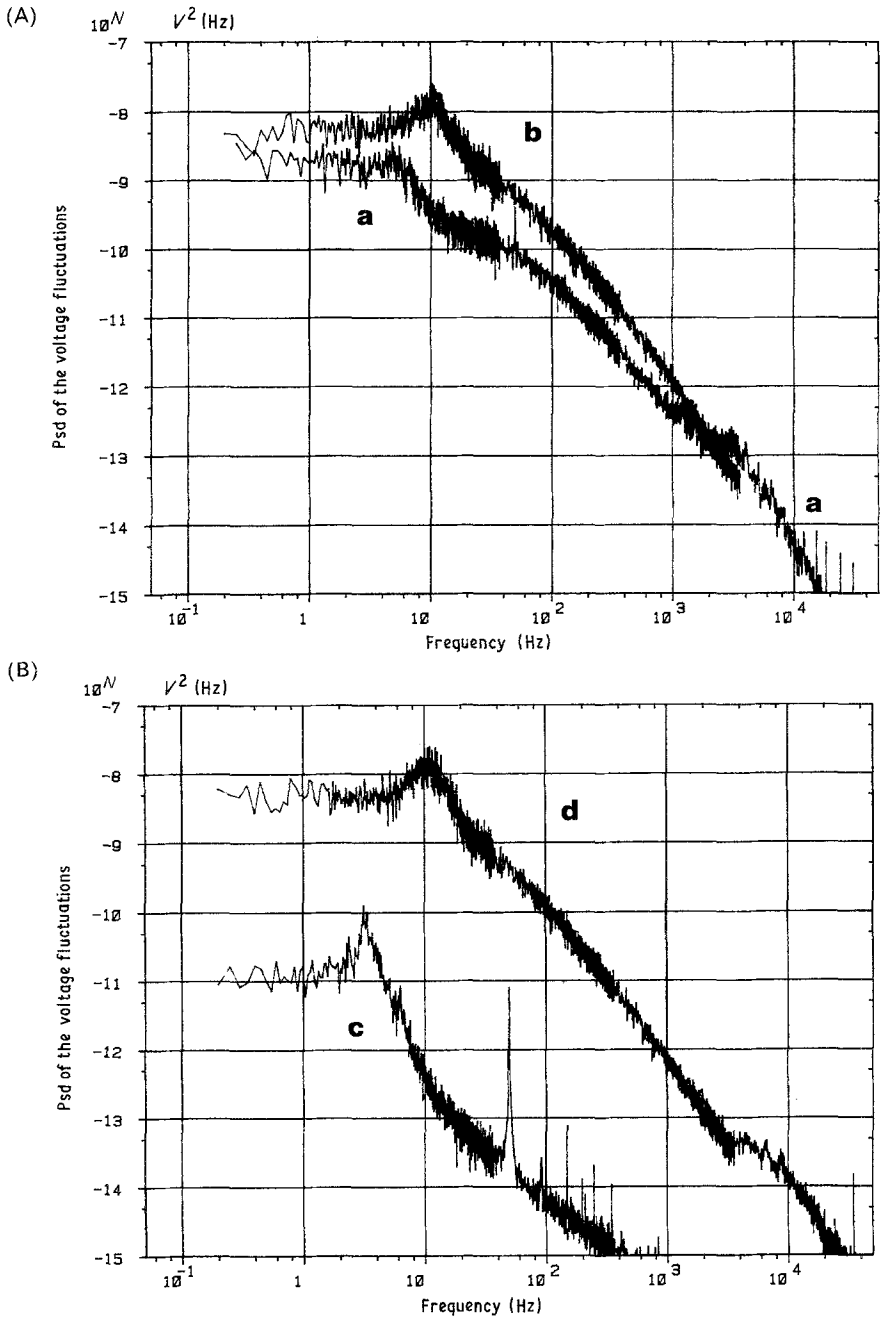

Fig. 5. Psd of the voltage fluctuations induced by gas evolution on a platinum disk electrode (diameter 0.5 mm) facing upwards in 1 M H_2SO_4. (A) Hydrogen evolution: (a) $J = 86\,mA\,cm^{-2}$; (b) $J = 382\,mA\,cm^{-2}$. (B) Oxygen evolution: (c) $J = 86\,mA\,cm^{-2}$; (d) $J = 864\,mA\,cm^{-2}$.

been plotted for low and high values of the electrolysis current density, J, in Fig. 5 for a sulphuric acid medium and in Fig. 6 for an alkaline one. All these spectra show a plateau in the low frequency range, a peak (better defined for oxygen than for hydrogen evolution in H_2SO_4, well defined for hydrogen and absent for oxygen evolution in NaOH) and a decrease in $f^{-\alpha}$ where α depends on the frequency range. At the beginning of the decrease the α value is close to 2 for the high electrolysis currents, and about 3 for the lower currents; in the highest frequency range all these spectra decrease with f^{-3}. A plateau is sometimes shown in the high frequency range, for example it is well defined for hydrogen evolution in NaOH medium; a possible explanation for this high-frequency plateau will be given in [11]. At last, for given gas and electrolyte, when the current density increases, the level of the psd and the frequency f_p of the peak also increase. Figures 5 and 6 show the great variety of the shapes of the measured spectra which reveals how much information about gas evolution they contain.

For calculating the characteristic parameters of the gas evolution, λ and $\langle \Delta\eta^2 \rangle$, from the measured spectra the previous model based on a renewal process with a pseudoperiodical distribution function of the time intervals between the bubble detachments has been used for oxygen and hydrogen evolution in H_2SO_4 and hydrogen evolution in NaOH, whereas the same model with an exponential distribution function has been used for oxygen evolution in NaOH where there is no peak in the spectra of the potential fluctuations. It must be noticed that, for low values of electrolysis current, the measured psd decreased approximately with f^{-3} after the low frequency

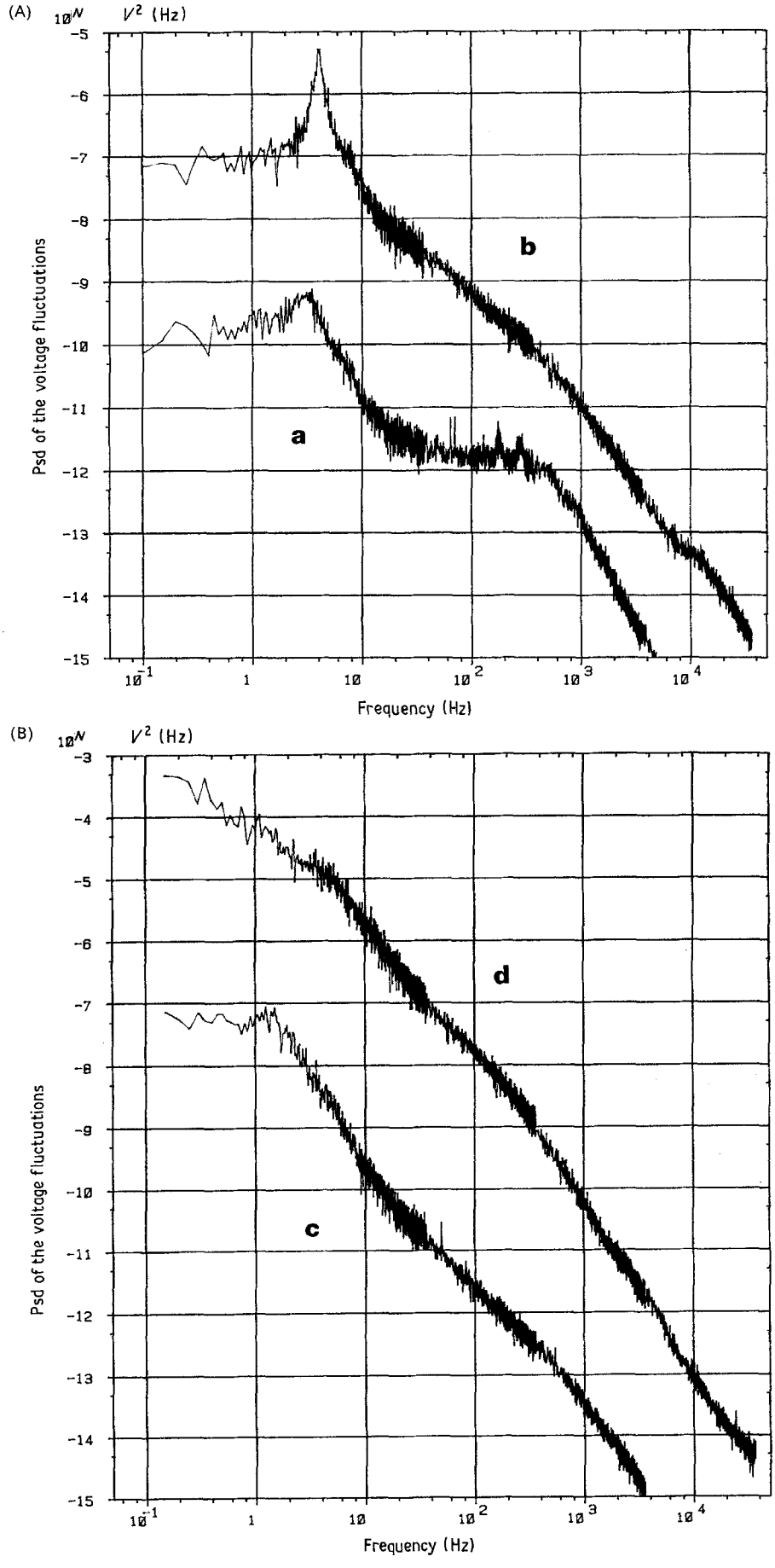

Fig. 6. Psd of the voltage fluctuations induced by gas evolution on a platinum disk electrode (diameter 0.5 mm) facing upwards in 1 M NaOH. (A) Hydrogen evolution: (a) $J = 81\,mA\,cm^{-2}$; (b) $J = 547\,mA\,cm^{-2}$. (B) Oxygen evolution: (c) $J = 83\,mA\,cm^{-2}$; (d) $J = 540\,mA\,cm^{-2}$.

plateau instead of f^{-2} in the model: in these conditions the theoretical and the measured spectra are in good agreement only for the low frequencies. On the other hand, for higher currents, the agreement is quite good over a wider frequency range, as for example oxygen evolution in H_2SO_4 (theoretical psd in Fig. 3, measured psd in Fig. 5B, curve d).

The bubble detachment frequency, λ, i.e. the number of bubbles evolved per unit time and the mean value, $\langle \Delta\eta \rangle$, of the amplitude of the potential jump due to a bubble detachment have been derived from the measured spectra by using Equation 23 , as indicated in Section 2, and are plotted in Fig. 7 for sulfuric medium and Fig. 8 for alkaline medium. From these figures, the dependence of λ on the current density, J, is given by the following proportionality relationship

$$\lambda \propto J^{\beta} \tag{31}$$

with $\beta = 1/3$, except for oxygen evolution in H_2SO_4 where $\beta = 1/2$. In Fig. 8B the only two experimental points nearly fit the straight line plotted with the slope

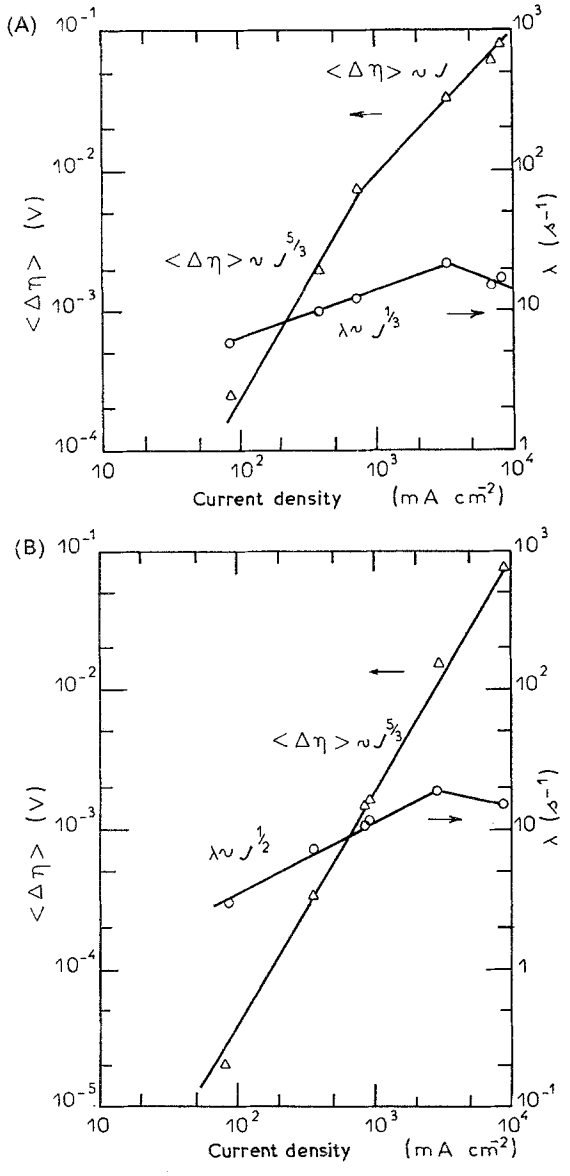

Fig. 7. Bubble detachment frequency λ and average amplitude $\langle \Delta\eta \rangle$ of the potential jump due to a bubble departure from a platinum disk electrode (diameter 0.5 mm) facing upwards in 1 M H_2SO_4. (A) Hydrogen evolution; (B) oxygen evolution.

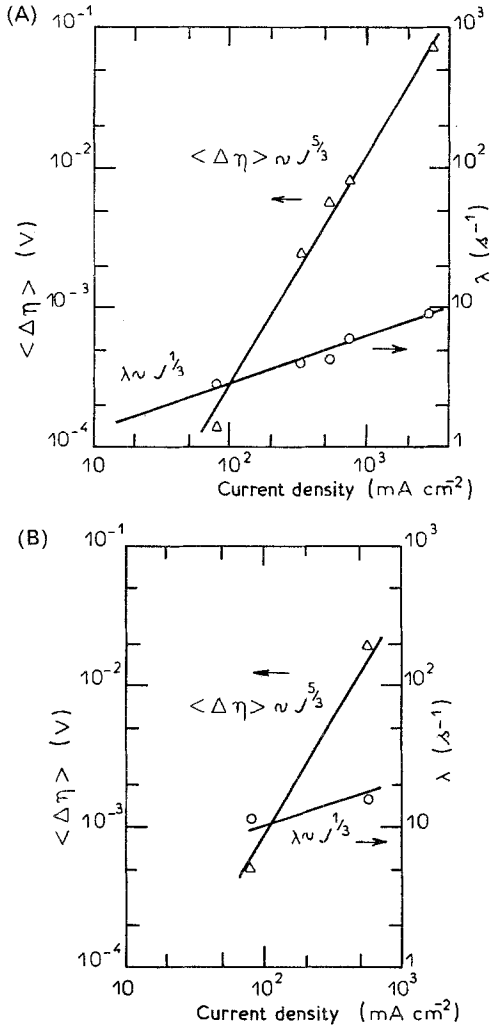

Fig. 8. Bubble detachment frequency, λ, and average amplitude, $\langle \Delta\eta \rangle$, of the potential jump due to a bubble departure from a platinum disk electrode (diameter 0.5 mm) facing upwards in 1 M NaOH. (A) Hydrogen evolution; (B) oxygen evolution.

$\beta = 1/3$ found for hydrogen evolution in acid and alkaline solutions; obviously more experimental results are necessary in order to validate this value of β. For the highest current densities ($J \geqq 3\,A\,cm^{-2}$), λ is independent of J in sulphuric medium. The increase of λ when the electrolysis current increased and the values of λ are in agreement with the optical observations made with the binocular microscope. The low values of λ, even for high current densities, show that the growth of the observable bubbles on the small electrode used cannot simply be controlled by diffusion of dissolved molecular gas: probably very numerous small bubbles grow on the electrode and disappear by coalescence with the bigger bubbles; the growth and the disappearance of these small bubbles are very fast, so that the growth of the few observable bubbles, whose number is limited by the small size of the electrode, is controlled essentially by coalescence of the small bubbles.

Possibly the observed potential fluctuations are due to the coalescence of bubbles which suddenly modifies the screened surface of the electrode, and so induces a steep potential jump (Equation 21). If r_1 and r_2 are the radii of two bubbles before their coalescence and r_3 is the radius of the resulting bubble after coalescence,

the screened surface of the electrode is proportional to $r_1^2 + r_2^2$ before coalescence and becomes proportional to r_3^2

$$r_3^2 = (r_1^3 + r_2^3)^{2/3}$$

after coalescence, if the gas volume is supposed constant. Thus for two bubbles of very different sizes, the screened surface is practically unchanged by coalescence, whereas in the worst case, for two identical bubbles, the screened surface decreases by a factor $1-2^{-1/3} = 20\%$. This shows that the amplitude of the potential jump induced by the coalescence of two bubbles is low compared to the amplitude of the potential jump due to a bubble departure. The potential fluctuations observed during gas evolution can then be ascribed to the detachment of the observable bubbles and not to the coalescence of the small bubbles.

Figures 7 and 8 also show that the mean value, $\langle \Delta\eta \rangle$, of the amplitude of the potential jumps due to the bubble detachments varied with $J^{5/3}$

$$\langle \Delta\eta \rangle \propto J^{5/3} \tag{32}$$

for hydrogen and oxygen evolutions in acid and alkaline solutions. Once again, for oxygen evolution in NaOH medium (Fig. 8B), only two experimental conditions have been investigated but the straight line, which was plotted with the same slope, 5/3, as for the three other evolution conditions, nearly fits the two experimental points. In the case of hydrogen evolution in H_2SO_4 medium, $\langle \Delta\eta \rangle$ increased linearly with J for high current densities ($J > 1\,A\,cm^{-2}$). It has already been noticed that the $\langle \Delta\eta \rangle$ derivation is valid even for non-linear potential transients, except for oxygen evolution in NaOH medium.

The mean value of the bubble detachment radius,

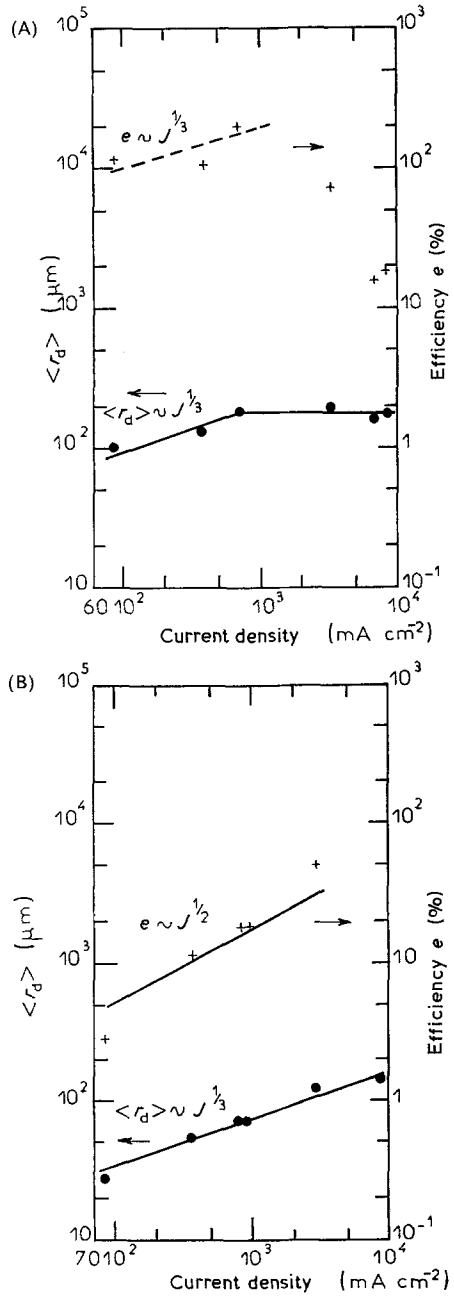

Fig. 9. Average bubble detachment radius $\langle r_d \rangle$ and gas evolution efficiency e (same conditions as in Fig. 7). (A) Hydrogen evolution; (B) oxygen evolution.

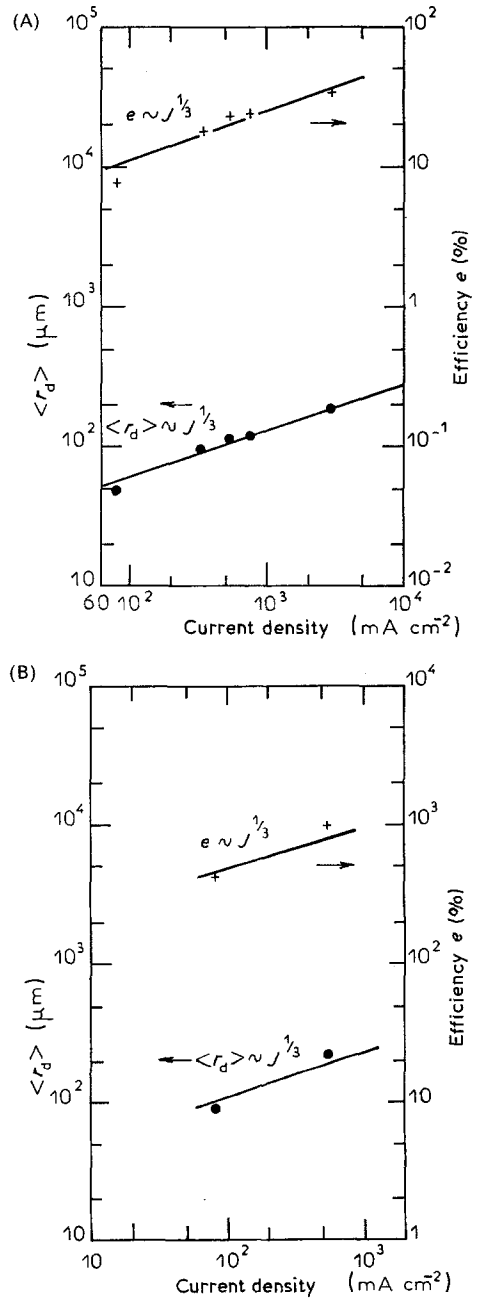

Fig. 10. Average bubble detachment radius $\langle r_d \rangle$ and gas evolution efficiency e (same conditions as in Fig. 8). (A) Hydrogen evolution; (B) oxygen evolution.

$\langle r_d \rangle$, and the gas evolution efficiency, e, derived from λ and $\langle \Delta\eta \rangle$ through Equations 23, 26 and 30, have been plotted in Fig. 9 for a sulphuric acid medium and Fig. 10 for an alkaline medium (the values of the electrolyte resistance are respectively $R_e = 25\,\Omega$ and $R_e = 58\,\Omega$). The straight lines plotted in Figs 9 and 10 correspond to straight lines of Figs 7 and 8 through Equations 26 and 30. From Equations 23, 26 and 32 it follows that $\langle r_d \rangle$ is proportional to $J^{1/3}$

$$\langle r_d \rangle \propto J^{1/3} \tag{33}$$

Figures 9 and 10 show that the radii of both hydrogen and oxygen bubbles in sulphuric and alkaline media vary with $J^{1/3}$ in the studied current density range, except for hydrogen bubbles in sulphuric medium at a high current density ($J > 1\,A\,cm^{-2}$) where $\langle r_d \rangle$ becomes independent of J. This may be explained by assuming the existence of a maximum bubble size (probably linked to the solution flow near the electrode due to bubble departures); this critical size would be reached by hydrogen bubbles and not by oxygen bubbles at the highest current density used ($9\,A\,cm^{-2}$) because of their smaller size. This increase of $\langle r_d \rangle$ with increasing electrolysis current and on the other hand the bigger size of hydrogen bubbles in sulphuric acid and of oxygen bubbles in sodium hydroxide at a given current density obtained in Figs 9 and 10, are results in agreement with the optical observations. The values of $\langle r_d \rangle$ given in these figures show a relatively good agreement with the results of Janssen *et al.* [16] obtained with a high-speed film camera on an oxygen-evolving nickel planar electrode in 1 M KOH medium. Those recently reported by Chin Kwie Joe *et al.* [17] are higher but the geometry of their electrode is quite different (thin wire electrode).

From Equations 30, 31 and 33, in the studied current density range, the gas evolution efficiency varies according to

$$e \propto J^{\beta} \tag{34}$$

where $\beta = 1/3$ except for oxygen evolution in sulphuric acid where $\beta = 1/2$. Figure 9 shows values of the hydrogen evolution efficiency of about 100% at low current densities and sometimes slightly higher values in the sulphuric medium. These high values have been measured over long times, therefore the efficiency cannot be overestimated as it would be over short times if bubbles were growing from previously supersaturated solution rather than merely by the faradaic process. The values higher than 100% are probably due to the approximations (Equations 23 and 24) assumed in this first attempt at derivation of the bubble efficiency from the measured psd of the potential fluctuations. In addition some quantities such as R_e, α_e, V_0 should be measured more precisely. At high current density ($J > 1\,A\,cm^{-2}$) the efficiency, which is proportional to $\lambda \langle r_d \rangle^3 / I$ (Equation 30), clearly decreases essentially because the average bubble detachment radius $\langle r_d \rangle$ does not increase further with increasing current as previously mentioned. For oxygen evolution Fig. 9 shows lower values of the gas bubble efficiency than for hydrogen evolution. These values increase when the electrolysis current increases and are low because the growth of the bubbles is essentially due to coalescence, which has been observed in our experiment (especially at low current density for middle-sized bubbles) to be easier for oxygen bubbles than for hydrogen bubbles in acid solutions. A greater part of the dissolved molecular gas produced at the electrode is then lost in the electrolyte.

In NaOH solution, it is well known that the coalescence of bubbles is much easier for oxygen bubbles than for hydrogen bubbles [16]. In the same way as before, this leads to low values of the hydrogen evolution efficiency, as shown in Fig. 10: the efficiency is almost the same as for oxygen evolution in sulfuric medium. On the other hand, it is also known [17] that in alkaline solution oxygen bubbles are more strongly attached to the electrode than hydrogen bubbles are: these two facts explain the much bigger size of oxygen bubbles which can be observed, and which is seen in Fig. 10. The values of the average radius, $\langle r_d \rangle$, of oxygen bubbles seem correct but the values of the efficiency which are derived from them are much too high. This is connected to the fact that the optical observations show a larger distribution of the detached bubble size for oxygen bubbles than for hydrogen bubbles. Thus the distribution function of the time intervals between two successive bubble departures is not pseudoperiodical but rather an exponential function. Under this assumption, the derivation of the parameters λ and $\langle \Delta\eta^2 \rangle$ from the measured psd of the potential fluctuations (Equation 11) is valid only for potential transients which are linear with time, which is not the case for bubbles whose growth is essentially controlled by coalescence. A further study is needed to obtain more relevant values of the gas evolution efficiency, in particular a statistical analysis could be done on the time recordings of the potential fluctuations in order to obtain a histogram of the amplitude of the steep potential jumps, i.e. a histogram of the bubble detachment radius, from which more realistic values of $\langle r_d \rangle$ and the efficiency, e, can be derived.

So far the potential fluctuations have been supposed not to be induced by coalescence of bubbles: this hypothesis has to be brought in question in the case of oxygen evolution in NaOH solution (and perhaps also for hydrogen evolution in sulphuric medium where slightly too high values of efficiency have been found) where coalescence is known to be an important phenomenon. The average number, λ, of steep potential jumps per unit time would be greater than the average number of bubble departures per unit time, since it also takes into account the coalescence of small bubbles, which would lead to a wrong estimation of $\langle r_d \rangle$. Further studies, for example by taking pictures of gas evolution with a high-speed film camera as in [16, 17] in order to obtain relevant values of the bubble detachment radii, are necessary to separate the contributions of the coalescence and the departure of bubbles on the potential fluctuations.

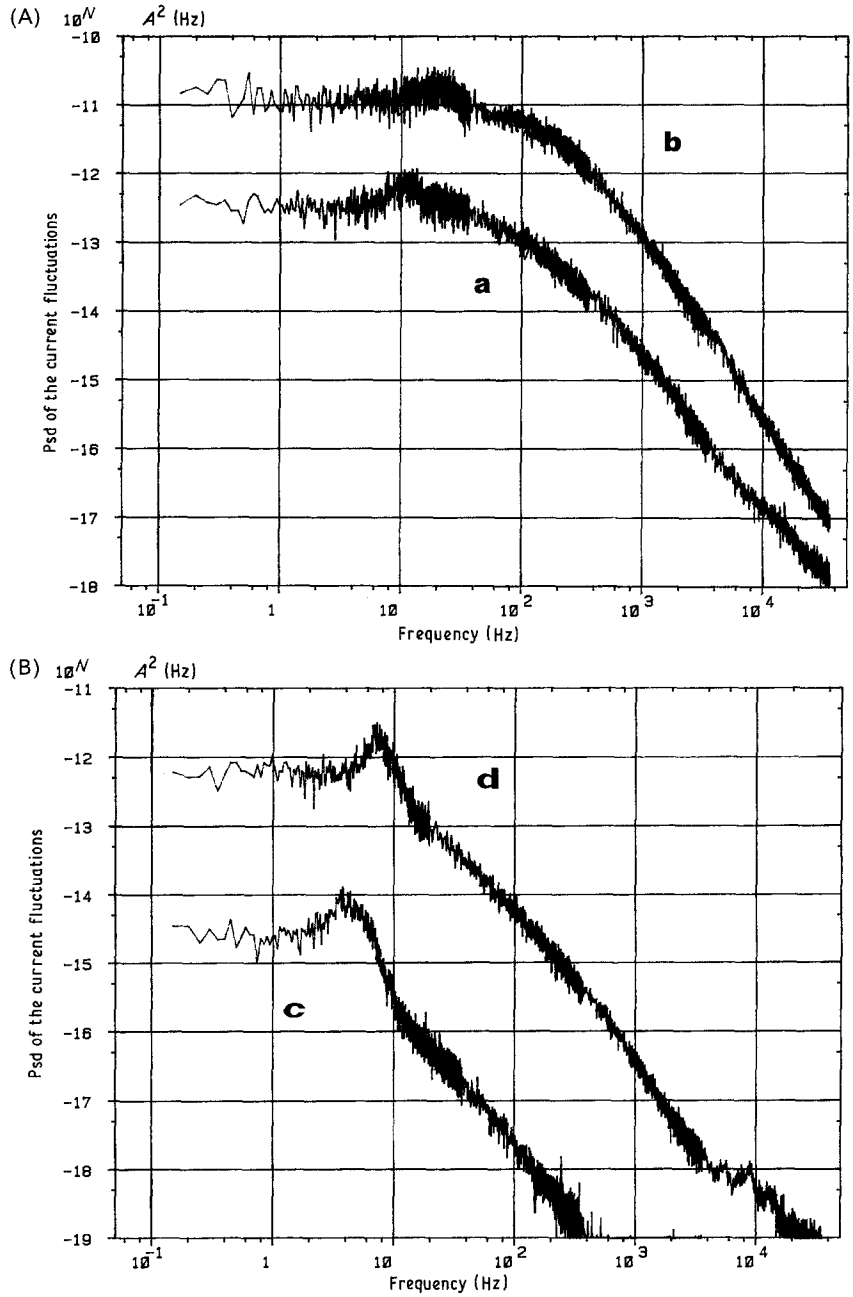

Fig. 11. Psd of the current fluctuations induced by gas evolution on a platinum disk electrode (diameter 0.5 mm) facing upwards in 1 M H_2SO_4. (A) Hydrogen evolution: (a) $J = 370\,mA\,cm^{-2}$; (b) $J = 1.4\,A\,cm^{-2}$. (B) Oxygen evolution: (c) $J = 160\,mA\,cm^{-2}$; (d) $J = 550\,mA\,cm^{-2}$.

It is difficult to compare the values of efficiency given in Figs 9 and 10 with the few values of the literature: some experimental values are given in [17] in KOH medium but the geometry of the working electrode is different (thin wire electrode). Vogt [18] calculated the theoretical efficiency of gas evolution with data in the literature on bubble growth or on supersaturation of electrolyte near the electrode: in sulphuric medium he found lower efficiency values than in Fig. 9 for hydrogen evolution and higher ones for oxygen evolution.

4.2. *Current fluctuations*

The psd $\psi_i(f)$ of the current fluctuations induced by oxygen and hydrogen evolution on the same platinum disk electrode (diameter 0.5 mm) facing upwards in 1 M H_2SO_4 solution were measured under potential control. The psd for a low and a high electrolysis current density have been plotted in Fig. 11. It can be seen that the general shape of these spectra is very similar to those of the potential fluctuations (low frequency plateau, peak more or less pronounced followed by a decrease in $f^{-\alpha}$, $\alpha > 0$ depending on the frequency range). This can be explained as the fluctuations of current and potential are induced by the fluctuations of the same physical quantity, that is the active surface of the electrode: the psd $\psi_i(f)$ and $\psi_v(f)$ are connected by the following relation [19]

$$\psi_i(f) = \frac{\psi_v(f)}{|Z(f)|^2} \tag{35}$$

where $Z(f)$ is the electrochemical impedance of the electrode at the studied polarization point.

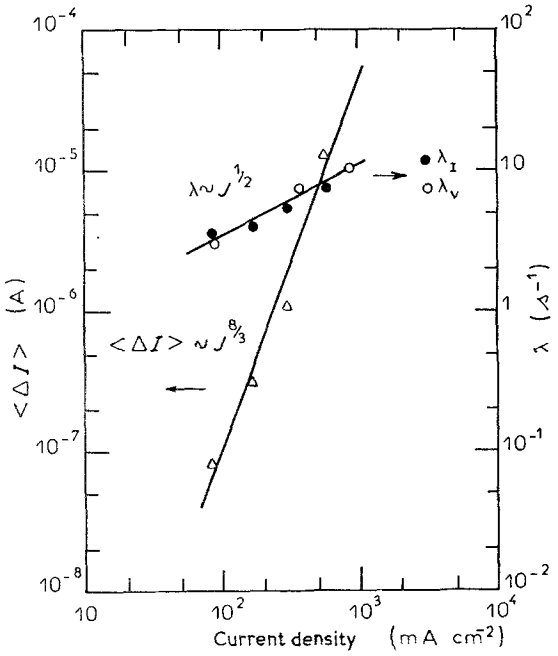

Fig. 12. Average amplitude $\langle \Delta I \rangle$ of the current jump due to a bubble detachment and bubble detachment frequencies λ_I, λ_V derived from the psd of respectively the current fluctuations and the voltage fluctuations (same conditions as in Fig. 11).

The psd of the current fluctuations due to oxygen evolution have been measured for different electrolysis current densities ranging from 80 to 600 mA cm^{-2}. As previously, owing to the model with a pseudoperiodical distribution function of the time intervals between successive bubble departures, the average bubble detachment frequency, λ, and the average amplitude of the steep current jump, $\langle \Delta I \rangle$, induced by a bubble departure have been derived and plotted in Fig. 12. These values of λ are in good agreement with those derived from the psd of the potential fluctuations which are also reported in Fig. 12. The average amplitude of the current jump, $\langle \Delta I \rangle$, is found to be proportional to $J^{8/3}$

$$\langle \Delta I \rangle \propto J^{8/3} \tag{36}$$

whereas the average amplitude of the potential jump, $\langle \Delta \eta \rangle$, was proportional to $J^{5/3}$. This difference can be explained by the following derivation which does not take into account the influence of the charge of the double layer capacity on the current jump. It has been shown by a complete calculation that this influence is negligible [10]. As a matter of fact this calculation, which is similar to the calculation of the dynamic overpotential due to a bubble growing on the electrode surface [9], shows that the variation of the double layer capacity, C, due to a bubble departure leads to an exponential variation of the electrolysis current with a time constant

$$\tau = C \frac{R_t R_e}{R_t + R_e} \tag{37}$$

where R_t and R_e are the charge transfer and electrolyte resistances before the bubble detachment. For a small electrode (diameter 0.5 mm) immersed in a high conductivity medium, such as our solutions, and the investigated current range, the following inequality holds

$$R_t \gg R_e \tag{38}$$

so

$$\tau = CR_e \approx 1\,\mu s \tag{39}$$

with $R_e \approx 25\,\Omega$ and $C \approx 40$ nF (20 μF cm^{-2}).

The current transient ($\propto \exp(-t/\tau)$) induced by the double layer capacity change due to a bubble departure is then very fast compared to the time scale of a few milliseconds corresponding to the bubble detachment. In the same way, for larger electrodes and/or low conductivity medium

$$R_e \gg R_t \tag{40}$$

the time constant

$$\tau = R_t C \tag{41}$$

is independent of the electrode size and is always very low. Therefore in all cases the influence of the double layer capacity change can be neglected.

The total overpotential, η_t, for a gas-evolving electrode can be written with Equations 2, 3 and 4 while still neglecting the concentration overpotentials

$$\eta_t(t) = R_e I + \Delta\eta_{ohm}(t) + \overline{\eta_{a,o}}(I) + \Delta\eta_a(t) \tag{42}$$

In this equation $\Delta\eta_{ohm}$ and $\Delta\eta_a$ are potential fluctuations due to bubble departures and the time-averaged ohmic component, $\overline{\eta_{ohm,o}}$, has been expressed by

$$\overline{\eta_{ohm,o}} = R_e I \tag{43}$$

where I is the electrolysis current and R_e the electrolyte resistance of the electrode covered with bubbles.

Under current control, the sudden detachment of a bubble instantaneously induces only a potential jump $\Delta\eta_{ohm}$: as a matter of fact the components $R_e I$ and $\overline{\eta_{a,o}}(I)$ are kept constant under current control and $\Delta\eta_a$, which represents the response of the kinetics of the molecular gas production reaction to the bubble configuration change on the electrode, takes some time to be established. The modulus of the mean value of $\Delta\eta_t$, previously denoted $\langle \Delta\eta \rangle$, is then written as

$$|\langle \Delta\eta_t \rangle| = |\langle \Delta\eta_{ohm} \rangle| = \langle \Delta\eta \rangle \tag{44}$$

Under potential control (η_t is kept constant), for the same reasons as before, a bubble departure induces a current change, ΔI, which does not instantaneously change $\Delta\eta_a$, but modifies the three other terms in Equation 42

$$\Delta\eta_t = 0 = R_e \Delta I + \langle \Delta\eta_{ohm} \rangle + \Delta\overline{\eta_{a,o}}(I) \tag{45}$$

The variation of the activation overpotential is given by Tafel's law

$$I \propto e^{b\overline{\eta_{a,o}}} \tag{46}$$

i.e.

$$\Delta\overline{\eta_{a,o}}(I) = \frac{1}{bI} \Delta I \tag{47}$$

or

$$\Delta\overline{\eta_{a,o}}(I) = R_t \Delta I \quad (48)$$

by introducing the charge transfer resistance, R_t, of the electrode covered with bubbles

$$R_t = \frac{\partial\overline{\eta_{a,o}}}{\partial I} = \frac{1}{bI} \quad (49)$$

The modulus of the average amplitude $\langle \Delta I \rangle$ of the current jump can then be expressed, with Equations 45 and 48, by

$$\langle \Delta I \rangle = \frac{\langle \Delta\eta \rangle}{R_e + R_t} \quad (50)$$

On the other hand, the electrolyte resistance is about 25 Ω and the order of magnitude of the parameter $1/b$ is 100 mV: thus for the studied current density range (80–600 mA cm^{-2}), it can be shown that

$$R_t \gg R_e \quad (51)$$

Equation 50 is then written with Equation 49

$$\langle \Delta I \rangle = \langle \Delta\eta \rangle \frac{I}{b}$$

As $\langle \Delta\eta \rangle$ varies with $I^{5/3}$, $\langle \Delta I \rangle$ is proportional to $I^{8/3}$ as shown in Fig. 12.

Thus the measurement of the psd of the current fluctuations corroborates the results obtained from the psd of the potential fluctuations, but the calculation of the parameters variation with current is more complicated.

Therefore, whenever the shape of the current–voltage curve enables it, it is better to polarize the gas-evolving electrode under current control and measure overpotential fluctuations.

5. Conclusion

The analysis of the potential or current fluctuations induced by a gas evolution on the electrode is proving attractive: merely in the frequency domain the great variety of the measured psd shows that they contain a lot of information about gas evolution, but further extensive work is required to interpret these spectra accurately.

In this paper, it has been shown for hydrogen and oxygen evolution in acid and alkaline solutions, that the low frequency part of the psd of the potential fluctuations represents the fluctuations of the electrode active surface, and that the growth of the bubbles on this electrode of dimension not much larger than the bubble sizes is essentially controlled by coalescence and not by the diffusion of the dissolved molecular gas. A theoretical model allows the derivation from these spectra of some parameters characteristic of the gas evolution, such as the average number of bubbles evolved per unit time, the average bubble detachment radius and the gas evolution efficiency.

These first results are hopeful, but further studies are necessary, in particular a statistical analysis on the time recordings of the potential fluctuations, to validate the parameter derivation. The analysis of the potential fluctuations in order to estimate the gas evolution parameters will then be a technique which, on the one hand is easier to employ than the classical use of a high-speed film camera, and on the other hand allows the gas evolution efficiency to be estimated at the electrode surface and not at a few millimeters above, as is usually done. If the bubbles were photographed while they were still attached to the electrode, i.e. while they were still growing, it would have been impossible to determine the mean detachment radius of the bubbles.

References

[1] H. Vogt, in 'A Comprehensive Treatise on Electrochemistry' (edited by E. Yeager, J. O'M. Bockris, B. E. Conway and S. Sarangapani), Plenum Press, New York (1981) Vol. 6, pp. 471–473.
[2] L. J. J. Janssen and E. Barendrecht, *Electrochim. Acta* **28** (1983) 341.
[3] A. T. Kuhn and M. Stevenson, *Electrochim. Acta* **27** (1982) 329.
[4] F. Hine, M. Yasuda, R. Nakamura and T. Noda, *J. Electrochem. Soc.* **122** (1975) 1185.
[5] J. A. Leistra and P. J. Sides, *J. Electrochem. Soc.* **134** (1987) 2442.
[6] J. Dukovic and C. W. Tobias, *J. Electrochem. Soc.* **134** (1987) 331.
[7] F. Job, PhD Thesis, Université de Grenoble, France (1979).
[8] C. Gabrielli, F. Huet and M. Keddam, *J. Appl. Electrochem.* **15** (1985) 503.
[9] C. Gabrielli, F. Huet, M. Keddam, A. Macias and A. Sahar, *J. Appl. Electrochem.* submitted.
[10] A. Sahar, PhD Thesis, Université de Paris VI, France (1988).
[11] C. Gabrielli, F. Huet, M. Keddam and A. Sahar, to be published.
[12] C. Gabrielli, F. Huet and M. Keddam, to be published.
[13] H. J. Larson and B. O. Shubert, 'Probabilistic Models in Engineering Science, Vol. II, Random Noise, Signals and Dynamic Systems', Wiley, New York (1979).
[14] C. Heiden, *Phys. Rev.* **188** (1969) 319.
[15] C. Gabrielli, F. Huet and M. Keddam, *Electrochim. Acta* **31** (1986) 1025.
[16] L. J. J. Janssen, C. W. M. P. Sillen, E. Barendrecht and S. J. D. Van Stralen, *Electrochim. Acta* **29** (1984) 633.
[17] J. M. Chin Kwie Joe, L. J. J. Janssen, S. J. D. Van Stralen, J. H. G. Verbunt and W. M. Sluyter, *Electrochim. Acta* **33** (1988) 769.
[18] H. Vogt, *Electrochim. Acta.* **29** (1984) 167.
[19] F. Huet, PhD Thesis, Université de Paris VI, France (1984).